IEEE Access
Multidisciplinary | Rapid Review | Open Access Journal

Received October 18, 2018, accepted November 5, 2018, date of publication March 6, 2019, date of current version March 18, 2019.

Digital Object Identifier 10.1109/ACCESS.2018.2883475

Effect of Linewidth Enhancement Factor on Fringe in a Self-Mixing Signal and Improved Estimation of Feedback Factor in Laser Diode

CHOLHYON KIM, CHOLMAN LEE, AND KWONHYOK O
KimChaek University of Technology, Pyongyang 950003, North Korea
Corresponding author: CholhyonKim (rcm6589@star-co.net.kp)

ABSTRACT The optical output power of a laser diode is modulated by the self-mixing effect when the optical beam is back-reflected or back-scattered into the laser cavity by a target. The optical feedback factor C is the most important one that defines the feature of the self-mixing signals (SMSs). And the estimation of C is indispensable for the displacement reconstruction by the phase unwrapping method because it is impossible to reconstruct the displacement with sub-wavelength resolution, provided the exact value of C is unknown. Unfortunately, C is subject to constant change during the measurement and, what is worse; its estimation is usually very time-consuming. This paper studies the feature of a high and low fringe of SMSs in moderate and strong feedback regime and the effect of the feedback factor and the linewidth enhancement factor on the fringes and presents a simple approach to the estimation of C when $C > 1.5$ based on the behavioral model proposed by Plantier *et al.* In particular, the novel approach enables fast direct estimation of C because it is based on analytic relations between C and the amplitudes of the high and low peak in SMSs.

INDEX TERMS Low-cost self-mixing sensor, optical feedback factor, fast estimation, laser diode, behavioral model.

I. INTRODUCTION

The self-mixing effect occurred by optical feedback has been widely used during the last three decades for displacement, velocity, distance and flow measurements, for the setup is simple and compact and particularly does not need difficult collimation and, therefore, it is very easy to use it. It is important to estimate the feedback factor C in real time in the measurement of the displacement. In fact, C is proportional to the distance and reflectivity of the target, thereby changing during the measurement of SMSs. In particular, C must be exposed to large variation when the target is non-corporative or the displacement is great [1], [2].

The waveform of SMSs depends mainly on the feedback factor C. The feedback regime can be classified to three regimes depending on the value of C [3], [4]: a weak feedback regime ($C < 1$); a moderate feedback regime ($1 < C < 4.6$); and a strong feedback regime ($C > 4.6$). An SMS takes sinusoidal shape in a weak regime and saw-toothed shape with hysteresis in moderate and strong regimes.

What is interesting in SMSs with hysteresis is the fact that the amplitude of a ''high peak'' is always lower than that of a ''low peak'' and their amplitudes decrease as C increases [2]. The high and low peaks constitute the SMS when the target moves away from and toward the LD, respectively. Fig. 1 shows the occurrence of the high and low peaks in SMSs with hysteresis. The high and low peak not only have different amplitudes but also opposite slopes, for the moderate and strong regime exhibit hysteresis. This hysteresis effect, which has been deeply studied, is due to the phase jump in the phase equation obtained from the Lang-Kobayashi equations [2], [5], [6]. But, unfortunately, there has not been an analysis of why the amplitude of the high peak is always lower than that of the low one and of how the feedback factor and the linewidth enhancement factor influence on their amplitudes. Actually the amplitudes of the peaks are directly concerned with C and therefore the determination of the C value requires the analysis of the relation between the amplitudes and C.

Another interesting matter in SMSs with hysteresis is the ''loss of peaks'' (or ''disappearance of peaks''), in which the peaks of the high and low fringes disappear with increase in C [2]. In other words, the peaks disappear in pairs whenever C reaches certain values. A single fringe in SMSs corresponds to a half-wavelength displacement of the target and

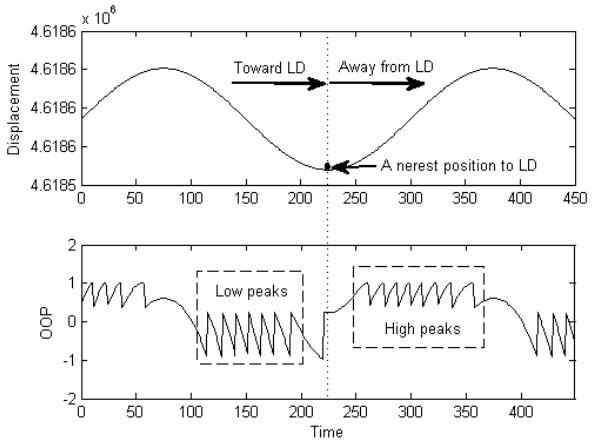

FIGURE 1. High peaks and low ones in an SMS with hysteresis. The high peaks occur when the target is moving toward an LD and the low peaks do when away from it.

therefore the total number of the fringes is proportional to the total displacement of the target. As a result the exact measurement of the displacement cannot be assured in the feedback regime with peak disappearance. But the accuracy of the displacement measurement can be secured even in the regime with peak disappearance if C is exactly measured, because the mechanism of the peak disappearance which occurs in the feedback regimes with hysteresis has been clarified in [2].

The shape of fringes in SMSs with hysteresis depends slightly or partly on the linewidth enhancement factor of an LD, too [2], [5], [6], and therefore its effect has to be taken into account for the estimation of C.

There have been proposed many methods of the estimation of C [1], [6]–[11]. These methods, however, are limited to a certain feedback level such as a weak or moderate regime and most of them except the method proposed in [6] need numerous samples for the estimation of C, which results in long time of calculation. Such a pity in these methods results mostly from not estimating C based on an analytic relationship between C and the so called interference function which expresses the shape of SMSs. Many models which describe the self-mixing effect have been presented and the behavioral model in [5] can be applied to all kinds of feedback regimes. The first order approximation in this model is relatively accurate and so it is used in a fast algorithm for the process of SMSs [5]. It is also possible to obtain the analytic relation of the effect of the feedback factor $C$and linewidth enhancement factor α on the amplitudes of the high and low peak by means of the first order approximation of the behavioral model.

In this paper we analyze the amplitude of peaks in SMSs with hysteresis based on the behavioral model of [5] and proposed a method of estimating C. In fact, the exact estimation of C is essential to reconstructing the displacement with sub-wavelength resolution by means of the phase unwrapping which is a very important technique for a displacement sensor based on the self-mixing effect [1], [7]. And an analytic relationship or simple algorithm for the estimation of C is very important to the real time and high-speed estimation of C especially in a low-cost embedded self-mixing sensor. Because our estimation method is based on the analytic relation to C, it is not only exact enough but also very simple, and therefore it will be very useful to the real time and high-speed estimation of C for a low-cost embedded self-mixing sensor with sub-wavelength resolution.

II. BASICS OF BEHAVIORAL MODEL

The self-mixing effect of an LD can be explained by the following phase equation obtained from the Lang-Kobayashi [5]

$$x_0(t) = x_F(t) + C\sin[x_F(t) + \arctan(\alpha)] = G[x_F(t); C, \alpha], \tag{1}$$

where x_F and x_0 are the phases of the external cavity with and without optical feedback, respectively, and are written as follows:

$$\begin{aligned} x_F(t) &= 2\pi \nu_F(t)\,\tau(t) \\ x_0(t) &= 2\pi \nu_0(t)\,\tau(t), \end{aligned} \tag{2}$$

where ν_F and ν_0 are the lasing frequencies with and without optical feedback, respectively, and $\tau(t) = 2D(t)/c$ is the round time of the external cavity, where $D(t)$ is the distance between the LD and the target which back-scatters a part of optical beam into the LD cavity and c the velocity of light in the external cavity. The inverse function of $G[x_F(t); C, \alpha]$ is written as

$$x_F(t) = F[x_0(t); C, \alpha] = G^{-1}[x_0(t); C, \alpha]. \tag{3}$$

The LD OOP is given as

$$P(t) = P_0\{1 + m\cos[x_F(t)]\}, \tag{4}$$

where P_0 is the OOP emitted by the free running state LD and m is the modulation index. The function $I = \cos[x_F(t)]$ is called the interference function which expresses the shape of a normalized SMS.

Our interest is the moderate and strong regimes with hysteresis, for the peak disappearance does not occur in a weak regime and therefore there is no need for the estimation of C in the measurement of displacement in this regime. Hence we study the feature of the fringe of SMSs and the estimation of C only for the regime with $C > 1$.

Fig. 2 shows the graph of $x_F = F[x_0(t); C, \alpha]$. The points $[x_{0,R}(k), x_{F,R}(k)]$ and $[x_{0,F}(k), x_{F,F}(k)]$ are the ones where the function $x_F = F[x_0; C, \alpha]$ has infinite slope and are given for even integers k as

$$\begin{aligned} x_{0,R}(k) &= k\pi - \arctan(\alpha) + \beta + C\sin(\beta) \\ x_{0,F}(k) &= (k+2)\pi - \arctan(\alpha) - \beta - C\sin(\beta) \\ x_{F,R}(k) &= k\pi - \arctan(\alpha) + \beta \\ x_{F,F}(k) &= (k+2)\pi - \arctan(\alpha) - \beta, \end{aligned} \tag{5}$$

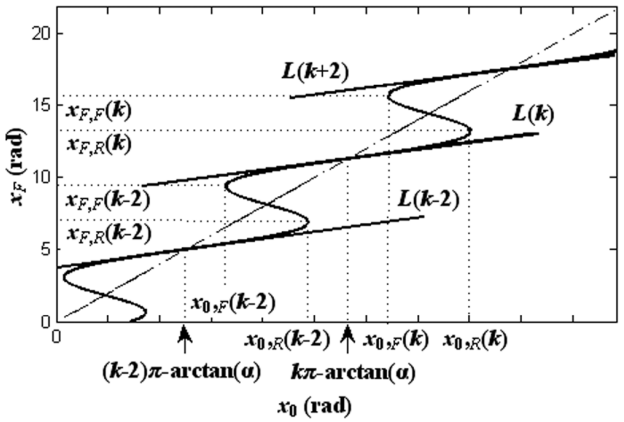

FIGURE 2. Plot of function $x_F = F[x_0; C, \alpha]$ when $C = 3$ and $\alpha = 3$. $L(k)$ with k even is the line tangent to the curve of the function $F[x_0; C, \alpha]$ at a point with coordinates $[k\pi - \arctan(\alpha), k\pi - \arctan(\alpha)]$.

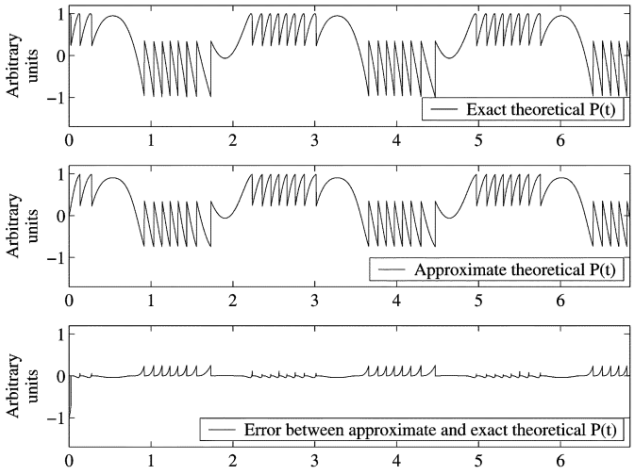

FIGURE 3. Simulation results of exact and approximate models with $C = 4.2$ and $\alpha = 3.4$ in [5]. The error between the two models occurs mainly at the discontinuities.

where

$$\beta = \arccos(-1/C). \tag{6}$$

[5] presented the approximate relation (7) between $x_0(t)$ and $x_F(t)$, which is the first order Taylor approximations of $F[x_0(t); C, \alpha]$ about $x_0(t) = k\pi - \arctan(\alpha)$.

$$x_F(t) \approx \frac{x_0(t) + (-1)^k C\,[k\pi - \arctan(\alpha)]}{1 + (-1)^k C} = \tilde{F}[x_0(t); C, \alpha] \tag{7}$$

The introduction of this approximation allows the function $F[x_0(t); C, \alpha]$ to be expressed by the straight lines $L(k)$ as shown in Fig.2. By the way, the first order approximation of the function $G[x_F(t); C, \alpha]$ is written as

$$x_0(t) \approx [1 + (-1)^k C][x_F(t) - k\pi + \arctan(\alpha)] + k\pi - \arctan(\alpha). \tag{8}$$

Fig. 3 shows the simulation result of the exact and approximate model for an experimental displacement presented in [5]. As shown in Fig. 3 both of the results are nearly same except the discontinuities. Hence, in the next sections we compare the amplitude of the high peak with that of the low one, analyze the effect of C and α on the amplitudes of the peaks and propose a method of the estimation of C based on the simple approximate model of [5] while we enhance the accuracy of the estimation of C through some compensation taking account of the errors between the exact model and the approximate model.

III. AMPLITUDES OF HIGH AND LOW PEAK

Fig. 4 shows the trajectory of the phase and "phase jumps" while the phase $x_0(t)$ lies between x_{0A} and x_{0B}.

In this case a point $[x_0(t), x_F(t)]$ follows the trajectory A, B, C, D, E, F and back to A while $x_0(t)$ passes from x_{0A} to x_{0B} and back to x_{0A}. The phase $x_F(t)$ jumps from B to C if the phase $x_0(t)$ becomes greater than

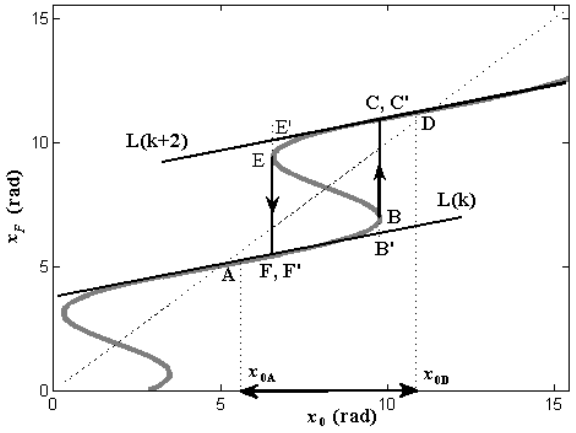

FIGURE 4. Trajectory of a phase point $[x_0(t), x_F(t)]$ of the function $F[x_0; C, \alpha]$ with $C = 3$ and $\alpha = 3$ and phase jumps at points B and E. The line $L(k)$ with k even is the first order approximation of the function $F[x_0; C, \alpha]$. The points B′ and F′ on the line $L(k)$ and the points C′ and E′ on the line $L(k+2)$ correspond to the points B, F, C and E on the curves of the function $F[x_0; C, \alpha]$, respectively.

$x_{0,R}(k) = k\pi - \arctan(\alpha) + \beta + C\sin(\beta)$ but jumps from E to F if it becomes smaller than $x_{0,F}(k) = (k+2)\pi - \arctan(\alpha) - \beta - C\sin(\beta)$.

(7) gives the ordinates of points B′, C′, E′ and F′ on the line $L(k)$ which is the first order of the function $F[x_0; C, \alpha]$. The ordinate $x_{F,B'}$ of B′ whose abscissa is $x_{0,R}(k) = k\pi - \arctan(\alpha) + \beta + C\sin(\beta)$ and the ordinate $x_{F,F'}$ of F′ whose abscissa is $x_{0,F}(k) = (k+2)\pi - \arctan(\alpha) - \beta - C\sin(\beta)$ on the line $L(k)$ are, respectively, given as

$$x_{F,B'} = k\pi - \arctan(\alpha) + \frac{\beta + C\sin(\beta)}{1 + C} \tag{9}$$

and

$$x_{F,F'} = (k+2)\pi - \arctan(\alpha) - \frac{\beta + C\sin(\beta)}{1 + C} - \frac{2\pi C}{1 + C}. \tag{10}$$

Likewise, the ordinate $x_{F,C'}$ of C′ and the ordinate $x_{F,E'}$ of E′ on the line $L(k+2)$ are, respectively, written as

$$x_{F,C'} = k\pi - \arctan(\alpha) + \frac{\beta + C\sin(\beta)}{1+C} + \frac{2\pi C}{1+C} \quad (11)$$

$$x_{F,E'} = (k+2)\pi - \arctan(\alpha) - \frac{\beta + C\sin(\beta)}{1+C}. \quad (12)$$

Now we analyze the features of the high and the low peaks. First, we examine why the amplitudes of the high and low peaks get lower with increase in C.

It is necessary to represent the interference function $I = \cos[x_F(t)]$ as the function of the phase $x_0(t)$ to obtain the peak amplitude.

As shown in Fig. 5, a single high peak appears when the phase $x_F(t)$ jumps from B to C in Fig. 4, thereby being written the amplitude of the high peak ΔI_h as

$$\begin{aligned}\Delta I_h &= I\left[x_{F,R}(k)\right] - I\left(x_{F,C}\right) = I\left(x_{F,B}\right) - I(x_{F,C}) \\ &= \cos\left(x_{F,B}\right) - \cos(x_{F,C}),\end{aligned} \quad (13)$$

where $x_{F,C}$ is the phase x_F at point C.

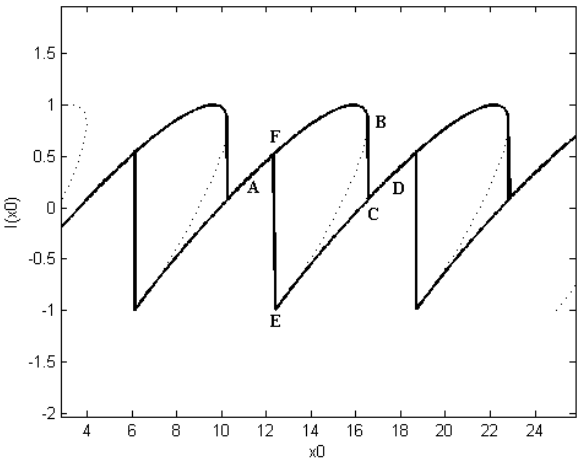

FIGURE 5. The interference function *I* plotted with respect to the phase $x_0(t)$. The dashed line is the mathematical solution of the function $I[x_0(t)]$ and the solid line the physical trajectory of it. Points A, B, C, D, E and F are the same as those in Fig. 4.

The first order approximate expression of ΔI_h can be determined by (9) and (11) as follows:

$$\begin{aligned}\Delta I_{h1st} &= \cos\left(x_{F,B'}\right) - \cos\left(x_{F,C'}\right) \\ &= \cos\left[-\arctan(\alpha) + \frac{\beta + C\sin(\beta)}{1+C}\right] \\ &\quad - \cos\left[-\arctan(\alpha) + \frac{\beta + C\sin(\beta)}{1+C} + \frac{2\pi C}{1+C}\right]\end{aligned} \quad (14)$$

Likewise, a single low fringe is produced due to the jump of the phase $x_F(t)$ from E to F and the first order approximation of its peak amplitude ΔI_l can be written by (10) and (12) as follows:

$$\begin{aligned}\Delta I_{l1st} &= \cos\left(x_{F,F'}\right) - \cos\left(x_{F,E'}\right) \\ &= \cos\left[-\arctan(\alpha) - \frac{\beta + C\sin(\beta)}{1+C} - \frac{2\pi C}{1+C}\right] \\ &\quad - \cos\left[-\arctan(\alpha) - \frac{\beta + C\sin(\beta)}{1+C}\right].\end{aligned} \quad (15)$$

The term $\frac{2\pi C}{1+C}$ in both (14) and (15) approaches 2π with increase in C. As a result, both the first order approximation of the amplitude of the high peak ΔI_{h1st} and the first order approximation of the amplitude of the low peak ΔI_{l1st} approach zero as the feedback factor C increases. This explains why both of the amplitudes of the high and low peaks in SMSs with hysteresis decrease as C increases.

Second, we compare the amplitude of the high peak with that of the low peak in order to explain why the former is always lower than the latter. For the sake of more exact explanation of it, (14) and (15) have to be modified. In fact, the difference between the ordinate $x_{F,R}(k)$ of the point B and the ordinate $x_{F,B'}$ of its first order approximation point B′ and the difference between the ordinate $x_{F,F}(k)$ of E and the ordinate $x_{F,E'}$ of its first order approximation point E′ can be determined by (5), (9) and (12), respectively, as

$$x_{F,R}(k) - x_{F,B'} = \beta - \frac{\beta + C\sin(\beta)}{1+C}$$

and

$$x_{F,F}(k) - x_{F,E'} = -\beta + \frac{\beta + C\sin(\beta)}{1+C},$$

which are relatively great in magnitude as shown Fig. 4. But the points C and F coincide with the points C′ and F', respectively, and therefore the differences of the ordinates x_F are very small. Table 1 shows the values of $|\Delta x_{F,CC'}| = |x_{F,C} - x_{F,C'}|$, $|\Delta I_{C,C'}| = |\cos(x_{F,C}) - \cos(x_{F,C'})|$, $|\Delta x_{F,FF'}| = |x_{F,F} - x_{F,F'}|$, $|\Delta I_{F,F'}| = |\cos(x_{F,F}) - \cos(x_{F,F'})|$ for different values of C and α, where $x_{F,F}$ is the phase x_F at point F and note $x_{F,F} \neq x_{F,F}(k)$. As shown in Table 1, $|\Delta x_F|$ depends only on C and does not do on α. Note that $|\Delta x_{F,CC'}|$ and $|\Delta I_{C,C'}|$ can be neglected when $C > 2$ because they are very small. Hence we can write much more exact expressions of the amplitudes of the high and low peak than (14) and (15), respectively, as

$$\begin{aligned}\Delta I'_{h1st} &= \cos\left[x_{F,R}(k)\right] - \cos\left(x_{F,C'}\right) \\ &= \cos\left[-\arctan(\alpha) + \beta\right] \\ &\quad - \cos\left[-\arctan(\alpha) + \frac{\beta + C\sin(\beta)}{1+C} + \frac{2\pi C}{1+C}\right]\end{aligned} \quad (16)$$

$$\begin{aligned}\Delta I'_{l1st} &= \cos\left(x_{F,F'}\right) - \cos\left[x_{F,F}(k)\right] \\ &= \cos\left[-\arctan(\alpha) - \frac{\beta + C\sin(\beta)}{1+C} - \frac{2\pi C}{1+C}\right] \\ &\quad - \cos\left[-\arctan(\alpha) - \beta\right].\end{aligned} \quad (17)$$

TABLE 1. Values of $|\Delta x_F|$ and $|\Delta I_{C,C'}|$ for different feedback factors and linewidth enhancement factors.

α	C	$\lvert\Delta x_{F,CC'}\rvert$	$\lvert\Delta I_{C,C'}\rvert$	$\lvert\Delta x_{F,FF'}\rvert$	$\lvert\Delta I_{F,F'}\rvert$
3	1	1.5708	0.6325	1.5708	1.2649
	1.5	0.2434	0.1421	0.2434	0.0045
	2	0.0767	0.0659	0.0767	0.0293
	3	0.0076	0.0075	0.0076	0.0057
	5	3.7601e-005	3.4828e-005	3.7601e-005	3.6365e-005
	7	0.0039	0.0032	0.0039	0.0039
	10	0.0192	0.0131	0.0192	0.0189
5	1	1.5708	0.7845	1.5708	1.1767
	1.5	0.2434	0.1165	0.2434	0.0257
	2	0.0767	0.0606	0.0767	0.0378
	3	0.0076	0.0074	0.0076	0.0063
	5	3.7601e-005	3.6317e-005	3.7601e-005	3.7270e-005
	7	0.0039	0.0034	0.0039	0.0039
	10	0.0192	0.0148	0.0192	0.0184

It is clear that (16) and (17) are the more exact expression than (14) and (15) to determine the amplitudes of the high and low peaks and therefore we will use these equations to estimate C.

As shown in (16) and (17) both of the amplitudes of the high and low peaks depend on C and α.

Fig. 6 shows the plots of the amplitude of the high peak $\Delta I'_{h1st}$ and of the amplitude of the low peak $\Delta I'_{l1st}$ with C for different values of α. As shown in Fig. 6, it turns out that the amplitude of the low peak $\Delta I'_{l1st}$ is always greater than the amplitude of the high peak $\Delta I'_{h1st}$ and both of them decrease greatly with increase in C.

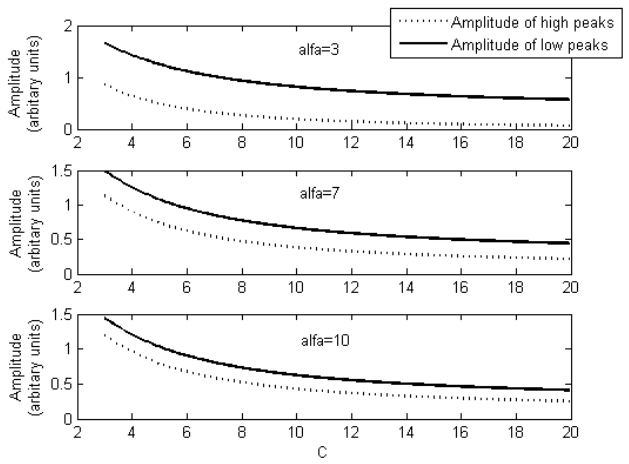

FIGURE 6. Comparison of amplitudes of high peak and low peak.

In fact the difference of both of the amplitudes is due to the presence of the linewidth enhancement factor. To be concrete, if it becomes zero in (16) and (17), the amplitude of the high peak $\Delta I'_{h1st}$ will be equal to the amplitude of the low one $\Delta I'_{l1st}$. The exact behavioral model in [5] gives the same consequence, too. As a result, it is the very the linewidth enhancement factor that makes the difference of both of the amplitudes.

In addition, it is interesting to note that the difference of both of the amplitudes is larger when α is smaller in Fig. 6.

IV. PREPARATION FOR ESTIMATION OF C

The interference function I can be expressed as the function of time when the target is in motion. The real-time estimation of C demands the direct estimation from an OOP signal, that is, the interference function $I(t)$. Hence, first of all, we study the characteristics of the interference function with the time t.

Assume that the target is in uniform motion. Actually targets are usually in sinusoidal motion in most of applications of self-mixing effect, but it will prove later that our assumption does not set a limit to solving the problem. Then the phase $x_0(t)$ can be written as

$$x_0(t) = 4\pi \frac{D_0}{\lambda_0} + 4\pi \frac{vt}{\lambda_0} \tag{18}$$

where D_0 is the initial distance of the target and λ_0 the wavelength of the LD without optical feedback.

As shown Fig. 7, the slope of the interference function increases with increase in the velocity of the target v.

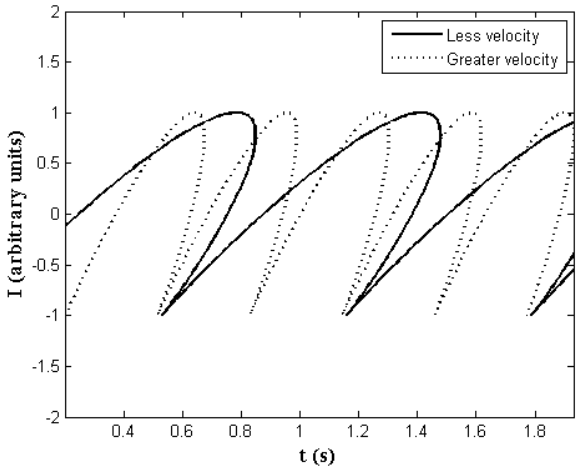

FIGURE 7. Interference function $I(t)$ for different velocities.

Using (7), the approximate derivative of the interference function I in terms of the time t at $x_0(t) = k\pi - \arctan(\alpha)$ is written as

$$\frac{dI}{dt} \approx \left(\frac{\partial I}{\partial x_F}\frac{\partial x_F}{\partial x_0}\frac{dx_0}{dt}\right)_{x_0 = k\pi - \arctan(\alpha)} = 4\pi \frac{v}{\lambda_0}\frac{1}{1+C}\sin(\arctan(\alpha)), \tag{19}$$

where k is even. The length Δt of the time interval $[t_1, t_2]$ corresponding to the interval $[x_0(k) = k\pi - \arctan(\alpha), x_0(k+2) = (k+2)\pi - \arctan(\alpha)]$ is given by (8) as

$$\Delta t = t_2 - t_1 = \frac{\lambda_0}{2v}. \tag{20}$$

From (19) and (20) the increment of the interference function ΔI corresponding to Δt is written as

$$\Delta I \approx 4\pi \frac{v}{\lambda_0} \frac{1}{1+C} \sin(\arctan(\alpha)) \cdot \frac{\lambda_0}{2v} = \frac{2}{1+C} \sin(\arctan(\alpha)). \quad (21)$$

(21) implies that the increment of the interference function ΔI does not depend on the velocity of the target and the lasing wavelength but does only on C and α. The observation of the derivation of (21) tells that the increment of the interference function I does not depend on the velocity of the target v even when the first order approximation is not applied. Consequently, the increment of the interference function and thereby the amplitudes are related only to C and α.

Now we discuss the way of estimating the feedback factor C based on the above consideration. As shown in Fig. 6, the amplitude of the high peak $\Delta I'_{h1st}$ and the amplitude of the low peak $\Delta I'_{l1st}$ are determined by C and α. It is possible to estimate C and α through (16) and (17) because both of the amplitudes of the high and low peaks can be found directly and simply from SMSs. The linewidth enhancement factor α is usually constant while C changes during the measurement of SMSs. Therefore, the important task is to estimate the feedback factor C rather than α. We use (16) and (17) to find the following equations for estimation of C.

Adding (16) to (17), we have

$$\Delta I'_{add} = \Delta I'_{h1st} + \Delta I'_{l1st} = 2\sin(\arctan(\alpha)) \cdot \left(\sin(\beta) - \sin\left(\frac{\beta + C\sin(\beta) + 2\pi C}{1+C}\right)\right). \quad (22)$$

Subtracting (16) from (17) gives

$$\Delta I'_{sub} = \Delta I'_{h1st} - \Delta I'_{l1st} = 2\cos(\arctan(\alpha)) \cdot \left(\cos(\beta) - \cos\left(\frac{\beta + C\sin(\beta) + 2\pi C}{1+C}\right)\right). \quad (23)$$

As shown in (22) and (23), the terms with the linewidth enhancement factor α are separated from the term with the feedback factor C. Combining (22) with (23), we can remove the term with α as follows:

$$\frac{(\Delta I'_{add})^2}{4\left(\sin(\beta) - \sin\left(\frac{\beta+C\sin(\beta)+2\pi C}{1+C}\right)\right)^2} + \frac{(\Delta I'_{sub})^2}{4\left(\cos(\beta) - \cos\left(\frac{\beta+C\sin(\beta)+2\pi C}{1+C}\right)\right)^2} = 1. \quad (24)$$

When obtaining (24), it was taken into account that

$$\sin^2(\arctan(\alpha)) + \cos^2(\arctan(\alpha)) = 1. \quad (25)$$

(24) without α and has the form of the elliptic equation. Consequently (16), (17), (23), (24) and (25) can be used for estimation of C, respectively.

V. SIMULATION AND EXPERIMENT

A. VERIFICATION OF THE PROPOSED METHOD FOR ESTIMATING C THROUGH SIMULATION

Fig. 8 shows the simulated SMSs with different values of C and a constant $\alpha = 3$. It is important to note Fig. 9 before discussing the method of estimating C by means of (16), (17), (22) and (23) for these SMSs, respectively. As shown in Fig. 9, the amplitudes of the high and low peaks involved in the proposed estimation method are slightly different from those obtained in the practical processing of the SMS. In fact, in our estimation method the amplitudes of the peaks are determined by the points, marked with an asterisk in Fig. 9, where the phase jumps, but in the practical processing of the SMS they are obtained by the maximum and minimum of the signal where the values of the interference function I are ± 1, respectively. Fortunately, the error of the estimation of C due to this difference can be improved through appropriate compensation.

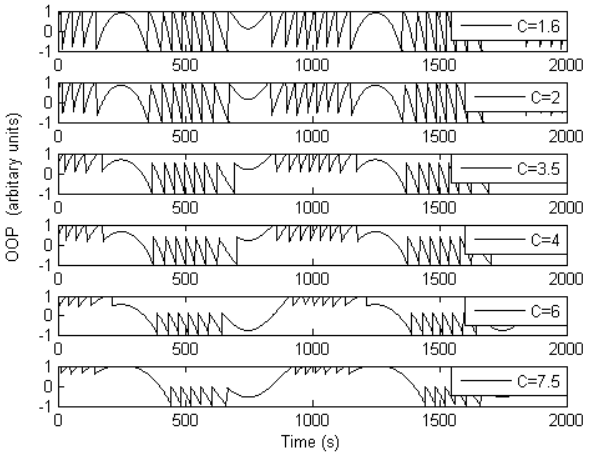

FIGURE 8. Simulated SMSs with C=1.6, 2, 3.5, 4, 6 and 7.5 and $\alpha = 3$.

Table 2 shows the results of the estimation of C by means of (16), (17), (22) and (23), respectively, for the simulated SMSs with different values of C. As shown in Table 3, the values estimated by (17) are the closest to the true ones and those by (23) the furthest from the true ones. The reason

TABLE 2. Estimation of C by using (16), (17), (22) and (23).

True C	C estimated by (16)	C estimated by (17)	C estimated by (22)	C estimated by (23)
1.6	0.65	1.25	0.75	-4.14
2	1.36	1.91	1.50	0.43
3.5	2.90	3.49	3.15	2.03
4	3.35	3.99	3.63	2.19
5	4.19	4.95	4.54	2.37
7	5.78	6.82	6.3	2.47
7.5	6.15	7.28	6.72	2.46
8.5	6.8	8.17	7.5	2.42
12	9.18	11.10	10.22	2.30

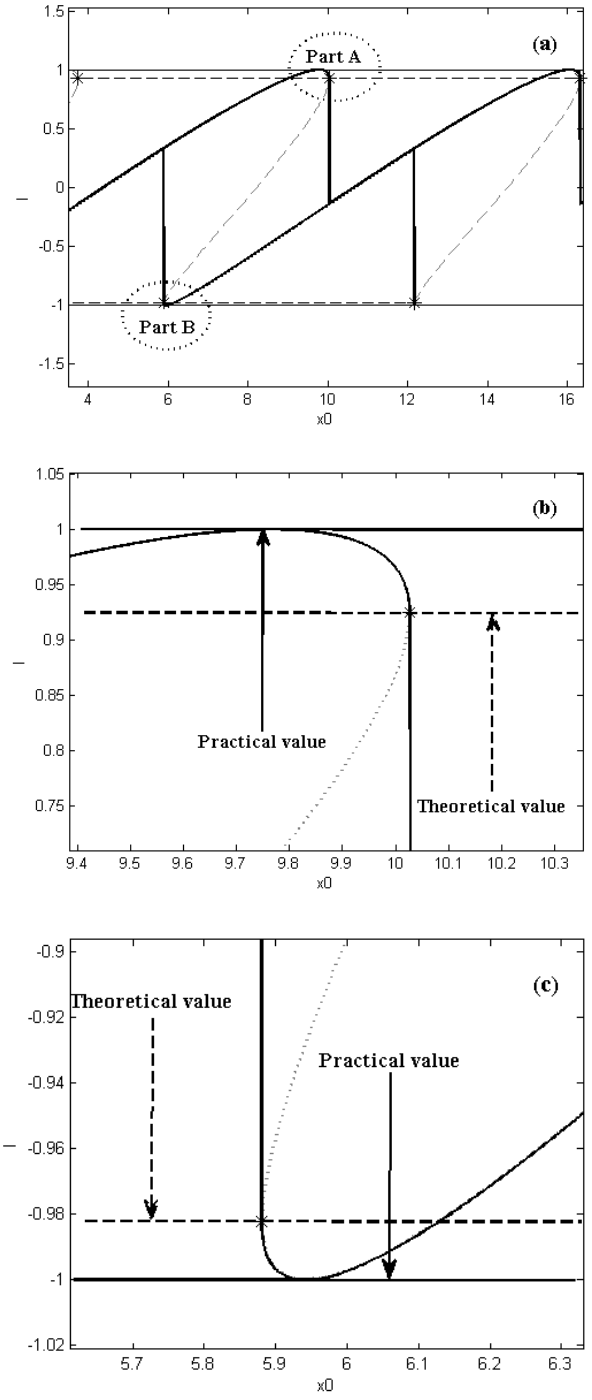

FIGURE 9. (a) Difference between our estimation method and the practical processing of the SMS in determining the amplitudes of the high and low peaks. (b) Zoom of the Part A in (a) which corresponds to the area of the high peak. (c) Zoom of the Part B in (a) which corresponds to the area of the low peak. The points marked with an asterisk are the points where the phase jumps. In our estimation method the values of the interference function at the phase jump points marked with an asterisk are used in the calculation of the amplitudes of the high and low peaks but in the practical processing of the SMS the maximum 1 and the minimum −1 of the interference function are used in the calculation.

why the errors of estimation by (16) are larger than those by (17) is because, in the processing of the SMS, the error in determining the amplitude of the high peak is always greater than the error in determining the amplitude of the low peak as shown in Fig. 9.

The estimation error is added to the error which results from the fact that this estimation method is based on the first order approximate model. But these errors can be improved by compensation. Our calculation proved that not only (17) but also (16) and (22) could afford the estimation of C with high accuracy when compensating through the interpolation. In the experimental verification of our estimation method below we estimate C based on the interpolation data obtained from this simulation results.

B. EXPERIMENT

Fig. 10 shows the experimental setup for the estimation of C. The setup contains an LD (model HL8325G, 820nm), a collimating lens, a variable attenuator to adjust the feedback factor C, a reflector as a target mounted on a loudspeaker which is driven by a sinusoidal signal at 210-Hz frequency. Reference [6] indicates the linewidth enhancement factor $\alpha = 3.2$ with an accuracy of $\pm 5.5\%$ in a HL8325G. According to our simulation and experiment, we found that the effect of the variation in α within its accuracy reported in [6] on the accuracy of C estimation could be neglected; therefore, we also used $\alpha = 3.2$ for the estimation of C by the experiment.

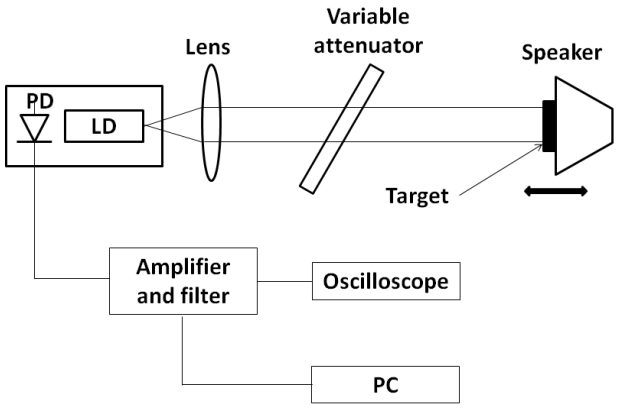

FIGURE 10. Setup for estimation of C. The variable attenuator can help to adjust the feedback factor.

Table 3 shows the comparison of the values of C estimated by the interpolation data based on (17) to those determined by a conventional data fitting technique for different

TABLE 3. Comparison of our estimation method and data fitting technique.

No	C estimated by our method	C estimated by a data fitting technique
1	1.63	1.71
2	2.40	2.38
3	3.67	3.69
4	5.54	5.54
5	7.47	7.48

SMSs obtained while changing the feedback level by the variable attenuator. The reason why we used (17) is that this equation is the best relationship for Cestimation as shown in Table 2. Every measurement result was obtained as an average of 10 times for the average amplitudes of the high and low peak over a period of the vibration of the target.

As shown in Table 3, both of the results coincide well and the new approach is simpler and much less time-consuming.

But note that because our estimation method is based on the analysis of the feature of the waveform of SMSs, it is affected by the signal-to-noise ratio like other estimation methods based on waveform analysis.

VI. CONCLUSION

In the paper we have studied the effect of the feedback factor C and the linewidth enhancement factor α on the amplitudes of the high and low peak in SMSs, based on the behavioral model in [5], and presented the analytic relations between C, α and the amplitudes of the peaks. From these relations, we have found that the linewidth enhancement factor caused the difference of the amplitudes of the high and low peak and explained why both of the amplitudes of the high and low peak decrease with increase in C and why the high amplitude is always smaller than the low one. In particular, we have proposed a novel approach to simpler and faster estimation of C with high accuracy for the moderate and strong feedback regime when C is greater than 1.5. The simplicity of our estimation method will be a great help to designing the software of an embedded system as well as the software of a personal computer-based system for a self-mixing displacement sensor with sub-wavelength resolution.

REFERENCES

[1] S. Merlo and S. Donati, "Reconstruction of displacement waveforms with a single-channel laser-diode feedback interferometer," *IEEE J. Quantum Electron.*, vol. 33, no. 4, pp. 527–531, Apr. 1997.

[2] J. E. Assad, "Analysis of self-mixing moderate and strong feedback regimes for mechatronics applications," Ph.D. dissertation, Toulouse Nat. Inst. Technol., Toulouse University, Toulouse, France, 2008.

[3] O. D. Bernal, U. Zabit, and T. Bosch, "Classification of laser self-mixing interferometric signal under moderate feedback," *Appl. Opt.*, vol. 53, no. 4, pp. 702–708, 2014.

[4] S. Donati, "Developing self-mixing interferometry for instrumentation and measurements," *Laser Photon., Rev.*, vol. 6, no. 3, pp. 393–417, 2012.

[5] G. Plantier, C. Bes, and T. Bosch, "Behavioral model of a self-mixing laser diode sensor," *IEEE J. Quantum Electron.*, vol. 41, no. 9, pp. 1157–1167, Sep. 2005.

[6] Y. Yu, G. Giuliani, and S. Donati, "Measurement of the linewidth enhancement factor of semiconductor lasers based on the optical feedback self-mixing effect," *IEEE Photon. Technol. Lett.*, vol. 16, no. 4, pp. 990–992, Apr. 2004.

[7] C. Bes, G. Plantier, and T. Bosch, "Displacement measurements using a self-mixing laser diode under moderate feedback," *IEEE Trans. Instrum. Meas.*, vol. 55, no. 4, pp. 1101–1105, Aug. 2006.

[8] U. Zabit, T. Bosch, and F. Bony, "A fast derivative-less optimization of the feedback coupling coefficient for a self-mixing laser displacement sensor," in *Proc. Joint IEEE North-East Workshop Circuits Syst. TAISA Conf.*, Jun./Jul. 2009, pp. 1–4.

[9] J. Xi, Y. Yu, J. F. Chicharo, and T. Bosch, "Estimating the parameters of semiconductor lasers based on weak optical feedback self-mixing interferometry," *IEEE J. Quantum Electron.*, vol. 41, no. 8, pp. 1058–1064, Aug. 2005.

[10] U. Zabit, "Optimisation of a self-mixing laser displacement sensor," Ph.D. dissertation, Toulouse Nat. Inst. Technol., Toulouse University, Toulouse, France, 2010.

[11] Y. Fan, Y. Yu, J. Xi, and J. F. Chicharo, "Improving the measurement performance for a self-mixing interferometry-based displacement sensing system," M.S. thesis, School Elect., Dept. Comput. Telecommun. Eng., Univ. Wollongong, Wollongong, NSW, Australia, 2011.

CHOLHYON KIM was born in Pyongyang, North Korea, in 1984. He received the M.S. and Ph.D. degrees in optical measurement from the KimChaek University of Technology, Pyongyang, in 2009 and 2018, respectively.

Upon graduation, he joined the Laser Engineering Department, KimChaek University of Technology, where he is currently a Professor.

CHOLMAN LEE received the B.S. and M.S. degrees in physical engineering from the KimChaek University of Technology, Pyongyang, North Korea, in 1994 and 1999, respectively, where he is currently pursuing the Ph.D. degree in laser engineering with the KimChaek University of Technology.

Since 1994, he has been a Professor with the KimChaek University of Technology. His research interests include semiconductor laser and optical measurement.

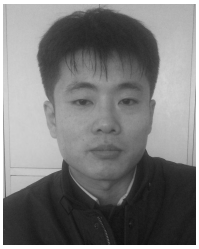

KWONHYOK O was born in Pyongyang, North Korea, in 1992. He received the B.S. and M.S. degrees in physical engineering from the KimChaek University of Technology, Pyongyang, in 2013 and 2016, respectively.

His research interests include quantum electronics and optical measurement.